KCC1 Activation protects Mice from the Development of Experimental Cerebral Malaria.

Elinor Hortle[1*], Lora Starrs[1*], Fiona Brown[2], Stephen Jane[2,4,5], David Curtis[2,4], Brendan J. McMorran[1], Simon J. Foote[1], and Gaetan Burgio[1]

Affiliations:

[1] Department of Immunology and Infectious Disease, John Curtin School of Medical Research, Australian National University. Australian Capital Territory, Australia

[2] Australian Centre for Blood Diseases, Central Clinical School, Monash University, Melbourne, Australia;

[4] The Alfred Hospital, Melbourne, Australia;

[5] Department of Medicine, Central Clinical School, Monash University, Melbourne, Australia

[*] These authors have contributed equally to this work

Corresponding author:

Dr Gaetan Burgio

The John Curtin School of Medical Research, The Australian National University

131 Garran Road, Canberra, ACT 2600, Australia

Gaetan.burgio@anu.edu.au

+61 2 612 59428

Abstract

Plasmodium falciparum malaria causes half a million deaths per year, with up to 9% of this mortality caused by cerebral malaria (CM). One of the major processes contributing to the development of CM is an excess of host inflammatory cytokines. Recently K+ signaling has emerged as an important mediator of the inflammatory response to infection; we therefore investigated whether mice carrying an ENU induced activation of the electroneutral K+ channel KCC1 had an altered response to *Plasmodium berghei*. Here we show that $Kcc1^{M935K/M935K}$ mice are protected from the development of experimental cerebral malaria, and that this protection is associated with an increased CD4+ T cells and TNF-α response. This is the first description of a K+ channel affecting the development of experimental cerebral malaria.

Introduction

Plasmodium falciparum malaria is a major cause of mortality worldwide, causing an estimated 219 millions cases and 435,000 deaths in 2018[1]. One of the most severe and lethal complications of *P. falciparum* infection is the sudden onset of seizures and/or coma, known as cerebral malaria (CM). Its occurrence varies from region to region, with a case fatality rate as high as 9% of severe malaria cases in some areas [2,3]. The causes of CM are not well understood, but hypotheses include the accumulation of parasitized red blood cells in the brain microvasculature, as well as imbalance in the pro- and anti- inflammatory responses to infection[4].

In recent years, potassium (K+) signaling has emerged as an important mediator of the immune response to infection. Several studies have shown *in vitro* that functional outwardly rectifying K+ channels are necessary for macrophage activation and production of TNFα[5,6], for activation of the NALP inflammasome[7], for the activation of T helper cells, and the formation of T regulatory cells [8-10]. The K+ content of the RBC also has a large effect on intra-erythrocytic *Plasmodium*. It has been shown that an outwardly directed K+ gradient is needed for normal parasite growth and maintenance of the parasite plasma membrane potential [11-13].

A mouse line expressing an activated form of K-Cl co-transporter type 1 (KCC1), discovered from a large scale ENU mutagenesis screen in mice, has recently been described[14]. The induced mutation – an M to K substitution at amino acid 935 of the protein – impairs phosphorylation of neighboring regulatory threonines, leading to over-activation of the transporter. The resulting increase in K+ efflux from the RBC causes *Kcc1*^{M935K} mice to display microcytic anemia, with homozygous mutants showing a 21% decrease in Mean Corpuscular Volume (MCV), 8% decrease in total hemoglobin, and 21% increase in number of red cells. Mutant cells are also significantly less osmotically fragile[14] indicating a dehydration of the red blood cells.

Here we use the *Kcc1*^{M935K} mouse line to investigate the effect of increased host K+ efflux on susceptibility to malaria infection. When *Kcc1*^{M935K} mice were infected with *Plasmodium berghei,* they showed protection from the development of experimental cerebral malaria (ECM), associated with a significant increase in CD4+ T cells and TNFα in the brain during infection, suggesting K+ efflux through KCC1 alters the

74 inflammatory response to infection. This is the first description of a cation co-
75 transporter affecting the development of ECM in mice.
76

77 **Results**
78

79 *Kcc1^{M935K} mice are protected against P. berghei infection*
80 Kcc1$^{M935K/M935K}$ mice were inoculated with *P. berghei* to determine their resistance to
81 parasitic infection. Cumulative survival and peripheral parasitemia were monitored
82 daily over the course of infection. When mice were infected with 1x10^4 *P. berghei*
83 parasitized red cells, survival was significantly increased in the mutants, with 100%
84 of homozygotes surviving past day 10 of infection, compared to 7% of WT females
85 (P=0.0004; Figure 1A), and 11% of WT males (P < 0.0001; Figure1B). Significantly
86 lower parasitemia was observed in both Kcc1^{M935K} females and males. In females,
87 parasitemia was reduced by 63% on day 7, 48% on day 8, and 42% compared to WT,
88 on day 9 post inoculation. Parasitemia in males was similarly reduced, by 66%, 41%,
89 and 53% respectively (Figure 1A-D).
90

91 To determine if this reduction in parasitemia was caused by impairment in the
92 parasite's ability to invade Kcc1$^{M935K/M935K}$ RBCs and survive within them, we
93 conducted TUNEL staining of infected RBCs to detect fragmented nuclei in the
94 parasites indicative of maturation arrest[15], and an *in vivo* invasion and maturation
95 assay as previously described[16]. No significant differences were observed in the
96 TUNEL assay (Figure 1E) but a significant 2-fold increase in parasitic growth for
97 Kcc1$^{M935K/M935K}$ RBCs at 13 hours (P < 0.001) and 21 hours (P < 0.001) (Figure 1F),
98 suggesting the Kcc1^{M935K} mutation does not affect parasite invasion but promotes

intra-erythrocytic survival. To explain increased intra-erythrocytic survival but lower parasitemia for Kcc1$^{M935K/M935K}$ over the course of infection (Figure 1B-D) we hypothesized that parasitic clearance was increased in the mutants. To address this postulate, we measured the proportion of labeled RBCs for WT and Kcc1$^{M935K/M935K}$ RBCs across time from 30 minutes to 24 hours post inoculation and found no difference in the proportion of remaining Kcc1$^{M935K/M935K}$ to WT labeled RBCs to WT indicative of no increase in parasitic systemic clearance and/or sequestration for Kcc1$^{M935K/M935K}$ RBCs.

In the experiments described above, 90% WT mice succumbed between days 8 and 10 post infection. Death at this point in *P. berghei* infection is usually caused by experimental cerebral malaria (ECM), and unrelated to the level of peripheral parasitemia. Combined with our results from the TUNEL and invasion assays, this hinted that the Kcc1^{M935K} mutation may not affect parasite growth, but may rather provide more systemic protection from ECM. We therefore infected mice with a dose of *P. berghei* at which 50% of WT mice survived beyond day 10 of infection. In this experiment Kcc1$^{M935K/M935K}$ had no difference in survival and no significant differences in parasitemia (Figure 1G-H). This suggests that parasite invasion or maturation is unlikely to be defective in Kcc1^{M935K} mutant mice.

Kcc1^{M935K} promotes resistance to ECM

To determine if the WT mice were succumbing to *P. berghei* infection in our challenges resulted from as a result of ECM, mice were injected with *P. berghei* and symptoms of ECM were scored according to severity, from 0 (no symptoms) to 5

(death). Severe clinical symptoms were observed in WT mice, with most dying from seizures, whereas Kcc1$^{M935K/M935K}$ remained asymptomatic for the length of the experiment (Figure 2A). One of the key hallmarks of cerebral malaria is breakdown of the blood brain barrier. Therefore, mice were injected intravenously with Evan's Blue to assess blood brain barrier integrity. Infected WT mice showed an average of 14.5±2.9 grams of dye per gram of brain tissue, which was higher than the 8.1±1.4g/g observed in uninfected mice. Infected Kcc1$^{M935K/M935K}$ more closely resembled uninfected mice, with 9.4 ± 1.3 g/g (Figure 2B-C). Although none of these differences was significant, the clear trend to higher staining in WT suggested a breakdown of the blood brain barrier that is not observed in Kcc1$^{M935K/M935K}$. ECM is also associated with increased sequestration of infected RBCs in the microvasculature. We therefore assayed the relative amount of parasite sequestration in the brain and spleen by PCR of *P. berghei* 18S RNA. Kcc1$^{M935K/M935K}$ showed a trend to decreased parasitemia in the brain, and increased parasitemia in the spleen (Figure 2D) indicating the difference in the ability of the parasite to cross the blood brain barrier. This trend was confirmed by measuring infected RBCs (iRBCs) in the brain by flow cytometry (Figure 2E). To further assess the postulate of an increase in sequestration of the parasitized RBCs in the brain tissue, we histologically assessed the presence of residual focal hemorrhages, oedema and neuropil changes in the brain tissue. At the pathological examination, the brain tissue appears normal for Kcc1$^{M935K/M935K}$ or WT mice (Figure 3A-C), with no presence of residual hemorrhages, petechies or oedema. However we found the presence of hemozoin pigmentation with significant disruption of the neuropil accompanied with white blood cells infiltrations and uninfected RBC infiltrates in the infected WT mice at day 10 post inoculation (Figure 3B), whereas this was not observed for infected Kcc1$^{M935K/M935K}$ mice (Figure 3D). Interestingly,

pathological examination of the spleen indicates no architectural differences between infected and uninfected Kcc1$^{M935K/M935K}$ and WT mice (Figure S1) but presence of hemozoin pigmentation in both strains indicates of splenic sequestration (Figure S1 C-D) and marked hyperproliferation of white blood cells in infected Kcc1$^{M935K/M935K}$ mice (Figure S1-D) which was not evident in the spleen of infected WT mice (Figure S1-C). Together with the clinical scores and Evan's blue staining, this suggests that WT mice are more likely to succumb to ECM due to a breakdown of the blood brain barrier and a moderate increase in iRBC population in the brain compared with Kcc1$^{M935K/M935K}$ which are more likely to be resistant to the development of this condition, possibly through an increased sequestration of parasites in the spleen, which also aids in preventing iRBC localization to the blood brain barrier.

Kcc1^{M935K} display an abnormal immune response to infection

It has been shown that depletion of CD4+ T cells, CD8+ T cells, and inflammatory monocytes can prevent the development of ECM [17-19]. ECM resistance is also observed in mice with impaired thymic development of CD8+ T cells[20]. Since the parasites were present in the brain and KCC1 is expressed ubiquitously[21], we postulated that the Kcc1^{M935K} mutation might cause alterations to some of these immune cell populations in the brain resulting in a stimulation of the immune response and impairment of parasite growth or increase clearance of the parasites. Therefore, the relative amounts of CD4+ and CD8+ T cells were measured by flow cytometry in the brain, blood, spleen, and thymus, both in uninfected mice, and the day the mice succumbed to ECM, where the inflammatory response is expected to be highest[22,23]. Consistent with the hypothesis that KCC1$^{M935K/M935K}$ mice are resistant to

174 ECM, differences in CD4+ and CD8+ T cells were observed in the brain (Figure 4 A-
175 B), but not in the blood, spleen, or thymus (Figures 4C-D and S2). When uninfected,
176 KCC1$^{M935K/M935K}$ showed a 4-fold increase in the average number of CD4+ T cells in
177 the brain compared to WT (Figure 3A). During infection, KCC1$^{M935K/M935K}$ had a
178 slight increase in the average amount of CD4+ T cells in the blood compared to WT
179 (Figure 4C). Importantly, KCC1$^{M935K/M935K}$ showed an 8-folds increase in CD4+ T
180 cells in the brain during infection ($P = 0.028$), compared to the CD4+ T cells in
181 infected WT, but only a 2-fold increase from their already higher baseline. The WT
182 mice did not show a change in CD4+ T cells in the brain during infection (Figure 4A).
183 Conversely, KCC1$^{M935K/M935K}$ had a 2.5-fold lower in CD8+ T cell count compared to
184 WT mice during infection ($p = 0.028$). There were no significant changes in CD8+ T
185 cells in either genotype from their baseline when placed under infection in the brain
186 (Figure 4B) or in the blood (Figure 4D).
187
188
189
190 One of the major host processes known to contribute to the development of cerebral
191 malaria in *P. berghei* infection is an over-active inflammatory response. Both *in vivo*
192 neutralisation of host molecules, and studies with knock-out mice have shown that
193 cerebral malaria can be prevented by depletion of the pro-inflammatory cytokines
194 IFN-γ [24,25] and TNFα [26], and can be induced by depletion of the anti-inflammatory
195 cytokine IL-10 [27]. ECM resistance is also observed in mice with defective T cell
196 dependent IFN-γ production [20]. We therefore measured cytokine levels in infected
197 mice in two ways: by ELISA in the brain and blood at a single time-point when all the

198 WT mice succumbed to ECM, so all mice were sacrificed; and by CBA array in the
199 plasma at several time-points over the first 10 days of infection.
200
201 At the single time-point, infected Kcc1$^{M935K/M935K}$ showed a significant 1.7-fold
202 increase in the average TNFα concentration in the brain (5723 pg/ml compared to
203 3329 pg/ml) and blood (2503 pg/ml compared to 1504 pg/ml) with a respective p-
204 value of 0.0068 in the brain and 0.0134 in the blood (Figure 5A), as well as a trend to
205 increased IL-1 β in the brain (Figure 5B). There were no differences in IFN-γ in
206 either the brain or blood at this time-point (Figure 5C). By CBA array,
207 Kcc1$^{M935K/M935K}$ showed no difference in plasma cytokine levels early in infection;
208 however, a 60% reduction in the amount of IFN-γ, and a 75% reduction in IL-6
209 were observed on day 9 of infection (391pg/ml compared to 969 pg/ml, and
210 2.4pg/ml compared to 10.3pg/ml respectively). This was followed by an 85%
211 reduction in the amount of IL-10 on day 10 of infection (an average of 8pg/ml in
212 Kcc1^{M935K} compared to 55pg/ml in WT) (Figure S3). A slight increase in the
213 amount of TNFα (P=0.040) was also observed on day 7 (Figure S3). Together this
214 indicates a possible protective effect of the Kcc1$^{M935K/M935K}$ mice against ECM by
215 altering the balance of IFN-γ and TNFα responses to infection.
216
217
218
219 **Discussion**
220
221 This study provides the first evidence that host KCC1 plays a role in malaria
222 resistance. It shows that over-activation of the transporter is likely to provide

223 protection to experimental cerebral malaria (ECM) in *P. berghei* infection. This is the
224 first description of a mutation in a cation transporter that has an effect on ECM; other
225 previously discovered genes have directly involved host cytokines, antigen
226 presentation [28,29], or erythrocyte membrane proteins [30-32].
227
228 Despite the fact that Kcc1$^{M935K/M935K}$ showed significantly lower parasitemia than WT
229 during the first 10 days of infection, the mutation did not appear to have a cell
230 autonomous effect on parasite invasion and survival within the RBC. One possible
231 explanation for this observation is suggested by the fact that *P. berghei* infected
232 RBCs have the ability to cytoadhere to the endothelium of blood vessels. Lower
233 levels of sequestration in the mutants would leave more late stage parasites vulnerable
234 to splenic clearance, and therefore result in reduced parasite burden[33]. Reduced
235 sequestration would also be consistent with protection from cerebral malaria, as
236 infected cells would be less likely to adhere within the microvasculature of the brain.
237 Our results from *P. berghei* 18S rRNA and histology examination support this
238 hypothesis, showing trends to reduced parasite burden in the brain and increased
239 burden in the spleen but were not significant due to the genetic variation amongst
240 mice.

241 Our results show increased CD4+ and decreased CD8+ T cells in the brains of
242 infected KCC1$^{M935K/M935K}$ compared with infected WT mice This corroborates
243 previous reports showing CD8+ are the major mediators of ECM[17], although it
244 remains unclear from these experiments why mutants would have altered T cell
245 populations in the brain even when uninfected. KCC1 is expressed on a wide range of
246 immune cells, and may greatly affect their function. Previous studies have shown that
247 K+ efflux can alter cellular cytokine production[5-7]; can increase assembly of the

NALP inflammasome in response to pathogen associated proteins[7]; and is essential for macrophage migration[34]. All of these may contribute to both T cell migration, and the increased IL-1β and TNF-α observed in KCC1^{M935K} mice.

The increase of pro-inflammatory cytokines in the brains of KCC1^{M935K} mice was surprising, as increased TNF-α have previously been associated with more severe CM (reviewed in [35,36]). However, it has been shown that neither TNF-α knock-out, or neutralization with antibodies, is sufficient to prevent CM [37,38], suggesting that the soluble cytokine is not itself causative of the condition. Although we did not find any significant differences in IFN-γ in the brains of KCC1^{M935K} mice at our single time point, we did observe a significant reduction in the plasma two days later than the significant increase in TNF-α. Interestingly, both IFN-γ knock-out and neutralization with antibodies, does protect against ECM (reviewed in [39]). It may therefore be that the KCC1^{M935K} mutation does not protect by modulation of any one cytokine, but by a better ability to quickly reduce inflammation after its initial peak.

Here we have shown that activation of KCC1 is likely to provide protection to *P. berghei* by preventing the development of experimental cerebral malaria (ECM). This is the first description of a mutation in a transporter that has an effect on ECM. Previous studies have shown that pharmacological activation of KCC channels is achievable[40,41], therefore future research into KCC1 activation may provide novel treatments for cerebral malaria.

Methods

Animals

Mice were bred under specific pathogen free conditions. All procedures conformed to the National Health and Medical Research Council (NHMRC) code of practice. All mouse procedures have been approved by the Australian National University Animal Experimentation Ethics Committee (AEEC A2014/054). The Kcc1^{M935K} mutation is carried on a mixed BALB/c and C57BL/6 background[14]. These two mouse strains differ in their susceptibility to *P. berghei*, and this introduced a greater amount of variability into results than is usually observed. Therefore, WT x WT and Kcc1$^{M935K/M935K}$ x Kcc1$^{M935K/M935K}$ breeding pairs were maintained. To exclude the possibility that the resistance phenotype was due to the mixed background, and carried by chance in mutant breeding pairs, Kcc1^{M935K} was periodically crossed back to WT, and new WT x WT and Kcc1$^{M935K/M935K}$ x Kcc1$^{M935K/M935K}$ pairs established from the progeny.

Infections

Experiments used the rodent parasite *P. berghei ANKA*. Parasite stocks were prepared from passage through resistant SJL/J mice, as described previously[42]. Experimental mice were infected intraperitoneally at a dose of $1x10^4$ or $1x10^5$ parasitised RBC per mouse. Blood stage parasitemia was determined by counting thin smears from tail blood stained in 10% Giemsa solution. A least 300 cells were counted per slide.

Histology

Uninfected, *P.berghei* infected mice and control were humanely euthanized. The brain was transcardially perfused by with 10 ml of 0.1M ice cold phosphate buffered saline solution (PBS) followed by 10 ml of ice cold 4% paraformaldehyde (PFA) and fixed into 70% ethanol. Brains and spleens from 5 mice from each group were serially

297 sectioned and stained with Hematoxilyn and Eosin (H&E). Brain and spleen sections
298 were independently examined from 2 different pathologists.
299 Thin tail smears from *P. berghei* infected mice were fixed in 100% MeOH, and
300 stained with an APO-BrdU TUNEL assay kit according to the manufacturer's
301 instructions (Invitrogen, Carlsbad, CA). Slides were examined on an upright
302 epifluorescence microscope (ZIESS) 600x magnification. 10 fields of view were
303 counted for each slide.
304
305
306 **Evans Blue**
307 *P. berghei* infected mice, and uninfected controls, were injected via IV with 200µl 1%
308 Evans Blue/PBS solution. 1hr post injection, mice were sacrificed and their brains
309 collected and weighed. Brains were placed in 2ml 10% neutral buffered formalin at
310 room temperature for 48hrs to extract dye. 200µl of formalin from each brain was
311 then collected and absorbance measured at 620nm. Amount of Evans blue extracted
312 per gram brain tissue was calculated using a standard curve ranging from 40µg/ml to
313 0µg/ml. Injections were carried out on the day of infection that the first mouse died.
314
315 **Clinical Score**
316 Mice were monitored three times daily, and given a score from 0 to 5 based on the
317 type and severity of their symptoms. '0' indicated no symptoms; '1' reduced or
318 languid movement; '2' rapid breathing and/or hunched posture; '3' ruffled fur,
319 dehydration and/or external bleeding; '4' fitting and/or coma; '5' death. Mice were
320 considered comatose if they were unable to right themselves after being placed on

their side. The highest score recorded for each mouse on each day was used to generate daily averages.

Cytokines

Peripheral blood was taken either by cardiac puncture or mandibular bleed in a microcentrifuge tube coated with anticoagulants and centrifuged for 4 minutes at 11,000xg. Plasma was then taken into a separate tube and stored at -20°C until needed. Cytokine analysis was conducted on un-diluted plasma using a CBA Mouse Th1/Th2/Th17 Cytokine Kit to the maker's instructions (BD biosciences).

Lymphocyte and Infected Red Blood Cell Analysis

Peripheral blood was taken either by cardiac puncture or mandibular bleed, and lymphocytes were isolated on Ficoll-Paque™ according to the maker's instructions. Lymphocytes were then incubated with Fc-block in MT-FACS for 10 minutes at 4°C.

Both spleen and thymus were prepared for flow cytometry using the same method. ½ of each organ was passed through a 70µm BD Falcon Cell Strainer with 0.5 ml of MT-FACS buffer, and then centrifuged at 300xg for 5 minutes at 4°C. The supernatant was removed and the pellet re-suspended in 5 ml cold MT-FACS buffer. A 200µl aliquot of this suspension was then incubated with 0.8µl Fc-block.

Blood, spleen and thymus samples were then stained with CD4-PacificBlue, CD11-PE, CD8-FITC, CD25-PECy7, CD19-PERCPCy5.5 and CD3-APC-Cy7, then fixed with 300µl of MT-PBS containing 1% formalin and 1% BSA for 10 minutes at 4°C. Cells were then permeabilised with MT-PBS containing 0.1% saponin and 1%BSA at

346 4°C for 20 minutes. Finally, cells were stained with FoxP3-APC. Samples were
347 acquired using a BD FACSAria™ II flow cytometer, and analysed using BD
348 FACSDiva™ software (BD Biosciences).

349 For comparative analysis of $CD3^+CD4^+$ and $CD3^+CD8^+$ brain lymphocyte populations
350 using flow cytometry, the brains of WT and mutant mice were harvested when WT
351 mice succumbed to ECM. Briefly, the entire brain was passed through a 70µm BD
352 Falcon Cell Strainer and collected post-straining in 1.5ml of PBS and then centrifuged
353 at 500xg for 5 minutes at 4°C. The supernatant from this was used for ELISA
354 (methods below). The cell pellet was then topped up to a total volume of 400µl with
355 PBS, and split as 300µl for FACs staining, and 100µl for PCR (methods below). The
356 samples were passed through a 70µm BD Falcon Cell Strainer again and then
357 centrifuged at 1500xg for 5 minutes at 4°C, prior to washing once with PBS; 10µl of
358 this pellet was then removed for infected RBC (iRBC) analysis. The remaining 40µl
359 cell pellet was blocked with 5µl Fc block for 10 minutes at 4°C. The pellet was then
360 washed twice with 200µl MTRC, and incubated with CD3-BV605, CD8-FITC and
361 CD4-APC antibodies. Samples were acquired at $2.5x10^6$ cells per sample, using a BD
362 LSRFortessa™, and analysed using BD FlowJo™ software.

363 The brain cell pellet previously removed for iRBC analysis, was incubated with TER-
364 119-PE-Cy7 antibody, with Hoechst 33342, and JC-1 dyes in MTRC, and $2.5x10^6$
365 cells were acquired per sample using a BD LSRFortessa™, and analysed using BD
366 FlowJo™ software.
367

368 **18s PCR from Brain, Spleen and Blood**

369 Brain samples were processed as described above. The spleen was also passed
370 through a 70µm BD Falcon Cell Strainer and resuspended to a total volume of 1.5ml

371 in PBS.

372

These cells were then centrifuged at 1500xg for 2 minutes at 4°C, and the supernatant was collected for ELISA (methods below). The pellet was resuspended to a total of 800µl and split in two, with 400µl taken for PCR, and 400µl snap frozen. Peripheral blood was collected using a cardiac puncture, and centrifuged at 1500xg 10 minutes at 4°C. The supernatant was taken for ELISA (below) and the pellet was lysed using two volumes of 0.15% saponin in PBS for 30 minutes at 37°C. Brain and spleen samples were processed similarly in order to successfully lyse any iRBC. The samples were then centrifuged at 10 000xg for 10 minutes at 4°C, and the pellet was washed three times with ice cold PBS. Following this, all samples were processed using the Qiagen DNeasy Blood and Tissue kit with following the manufacturer's instructions. The quality and yield of DNA was quantified using a NanoDrop spectrophotometer. 200ng of each sample was set up in a PCR reaction with 1x MyTaq™ Mix and 0.4 µM of GAPDH primers (Forward: GATGCCCCCATGTTTGT; Reverse: TGGGAGTTGCTGTTGAAG), or 0.4µM of 18s primers (Forward: CAGACCTGTTGTTGCCTTAAAC; Reverse: GCTTGCGGCTTAATTTGACTC). The reaction parameters for GAPDH were as follows, 95°C for 5 minutes before 35 cycles of 95°C 30 seconds, 50°C 30 seconds, 72°C 1 minute, and a final extension at 72°C 2minutes. Since the genome of *P. berghei* is AT rich, the PCR protocol for 18s was 95°C 5 minutes, before 35 cycles of 95°C for 30 seconds, 50°C for 1 minute, 68°C for 2 minutes, and a final extension of 68°C for 5 minutes. These reactions were then eletrophoresed on a 1% agarose gel, and imaged using a Bio-Rad Gel Doc™ XR+ Gel Documentation System. Densitometry analysis was conducted on these bands using ImageJ software, and standardized to GAPDH densitometry analysis.

ELISA from brain and blood

Samples were processed as described above, with the supernatants removed and saved for ELISA. ELISAs were conducted following the manufacturers' protocols, with the IL-1b and IFN-y (ELISAKIT.com, EK-0033 and EK-0002, respectively) and TNF-a (ThermoFisher Scientific KMC4022). Samples were diluted 1 in 5 and 1 in 10 for IL-1b; 1 in 4 and 1 in 8 for IFN-y, and 1 in 10 and 1 in 20 for TNF-α. The pdata was collected using a Tecan M200 plate reader.

In-vivo Invasion Assay

Blood from Mutant and WT uninfected mice was collected by cardiac puncture. 1800 μl of blood was collected and pooled for each genotype, then halved and stained with either NHS-Atto 633 (1 μl/100 μl) or sulfobiotin-LC-NHS-Biotin (1 μl/100 μl of 25mg/ml in DMF). Cells were then incubated at RT for 30 minutes, and washed twice in MT-PBS. Stained cells were combined in equal proportions to achieve the following combinations:

1) WT-Biotin + Mutant-Atto 2) WT-Atto + Mutant Biotin

Combined cells were then resuspended in 2ml MT-PBS, and injected intravenously into 4 WT *P. berghei* infected mice at 1-5% parasitemia, plus 1 uninfected control, were injected with 200 μl dye combination 1; the same numbers of mice were injected with 200 μl dye combination 2. Injections were carried out when parasites were undergoing schizogeny, at ~1am.

30 minutes post injection, 1 μl tail blood was collected and stained for 30 minutes at 4°C in 50 μl MT-PBS containing 0.25 μl CD45-APC-Cy7, 0.25 μl CD71-PE-Cy5,

0.5 μl Step-PE-Cy7. Next, 400 μl MTPBS containing 0.5 μl Hoechst 33342 and 1 μl 800 μg/ml Thiazole orange was added, and cells were incubated for a further 5 minutes at 4°C. Stained cells were then centrifuged at 750xg for 3 minutes, re-suspended in 700µl MT-PBS, and analyzed on a BD Fortessa Flow Cytometer. $2x10^6$ cells were collected for each sample, and data was analysed using FlowJo (FlowJo, LLC, Oregon, USA).

Statistical analysis

P values were determined using Log-rank test, Welch's T test or ordinary one- or two-way ANOVA where appropriate. Statistics on the clinical score (Figure 2A) was determined using two-stage linear step-up procedure of Benjamin, Krieger ad Yekutieli with Q=1%.

Acknowledgement

We would like to acknowledge Shelley Lampkin and Australian Phenomics Facility (APF) for the maintenance of the mouse colonies. This study was funded by the National Health and Medical Research Council of Australia (Program Grant 490037, and Project Grants 605524 and APP1047090), the National Collaborative Research Infrastructure Strategy (NCRIS), the Education Investment Fund from the Department of Education and Training, the Australian Phenomics Network, Howard Hughes Medical Institute and the Bill and Melinda Gates Foundation. This study utilizes the Australian Phenomics Network Histopathological and Organ Pathology service, University of Melborne. We finally would like to thank Dr John Finnie, University of Adelaide, Australia and Professor Catriona A. McLean from the University of

Melbourne, Australia for their assistance. We finally wish to acknowledge two anonymous reviewers for the careful reading of the manuscript and their helpful suggestions to improve the quality of this work.

Author Contribution Statement

E.J.H, B.J.M, S.F.J and G.B designed and planed the experimental work. E.J.H, L.S and F.C.B performed the research. E.J.H, S.M.J, D.J.C. B.J.M, S.F.J and G.B interpreted and analyzed the data. E.J.H, L.S. and G.B performed the statistical analysis. E.J.H, L.S and G.B wrote the manuscript. All authors reviewed the manuscript.

Competing Financial Interests

The authors declare no competing financial interests.

1 WHO. World Malaria Report. 161 (World Health Organization, 2018).

2 Grau, G. E. & Craig, A. G. Cerebral malaria pathogenesis: revisiting parasite and host contributions. *Future microbiology* **7**, 291-302, doi:10.2217/fmb.11.155 (2012).

3 Rockett, K. A. *et al.* Reappraisal of known malaria resistance loci in a large multicenter study. *Nat Genet* **46**, 1197-1204, doi:Doi 10.1038/Ng.3107 (2014).

4 Brooks, H. M. & Hawkes, M. T. Repurposing Pharmaceuticals as Neuroprotective Agents for Cerebral Malaria. *Curr Clin Pharmacol*, doi:10.2174/1574884712666170704144042 (2017).

5 Qiu, M. R., Campbell, T. J. & Breit, S. N. A potassium ion channel is involved in cytokine production by activated human macrophages. *Clin Exp Immunol* **130**, 67-74 (2002).

6 Ren, J. D. *et al.* Involvement of a membrane potassium channel in heparan sulphate-induced activation of macrophages. *Immunology* **141**, 345-352, doi:10.1111/imm.12193 (2014).

7 Petrilli, V. *et al.* Activation of the NALP3 inflammasome is triggered by low intracellular potassium concentration. *Cell Death Differ* **14**, 1583-1589, doi:10.1038/sj.cdd.4402195 (2007).

8 Bittner, S. *et al.* Upregulation of K2P5.1 potassium channels in multiple sclerosis. *Ann Neurol* **68**, 58-69, doi:10.1002/ana.22010 (2010).

9 Fellerhoff-Losch, B. *et al.* Normal human CD4(+) helper T cells express Kv1.1 voltage-gated K(+) channels, and selective Kv1.1 block in T cells induces by itself robust TNFalpha production and secretion and activation of the NFkappaB non-canonical pathway. *J Neural Transm (Vienna)* **123**, 137-157, doi:10.1007/s00702-015-1446-9 (2016).

10 Wulff, H. *et al.* The voltage-gated Kv1.3 K(+) channel in effector memory T cells as new target for MS. *J Clin Invest* **111**, 1703-1713, doi:10.1172/JCI16921 (2003).

11 Staines, H. M., Ellory, J. C. & Kirk, K. Perturbation of the pump-leak balance for Na(+) and K(+) in malaria-infected erythrocytes. *Am J Physiol Cell Physiol* **280**, C1576-1587 (2001).

12 Brand, V. B. *et al.* Dependence of Plasmodium falciparum in vitro growth on the cation permeability of the human host erythrocyte. *Cellular physiology and biochemistry : international journal of experimental cellular physiology, biochemistry, and pharmacology* **13**, 347-356, doi:75122 (2003).

13 Allen, R. J. & Kirk, K. The membrane potential of the intraerythrocytic malaria parasite Plasmodium falciparum. *J Biol Chem* **279**, 11264-11272, doi:10.1074/jbc.M311110200 (2004).

14 Brown, F. C. *et al.* Activation of the erythroid K-Cl cotransporter Kcc1 enhances sickle cell disease pathology in a humanized mouse model. *Blood* **126**, 2863-2870, doi:10.1182/blood-2014-10-609362 (2015).

15 McMorran, B. J. *et al.* Platelets kill intraerythrocytic malarial parasites and mediate survival to infection. *Science* **323**, 797-800, doi:10.1126/science.1166296 (2009).

16 Lelliott, P. M., McMorran, B. J., Foote, S. J. & Burgio, G. In vivo assessment of rodent Plasmodium parasitemia and merozoite invasion by flow cytometry. *J Vis Exp*, e52736, doi:10.3791/52736 (2015).

17 Claser, C. *et al.* CD8+ T cells and IFN-gamma mediate the time-dependent accumulation of infected red blood cells in deep organs during experimental cerebral malaria. *PLoS One* **6**, e18720, doi:10.1371/journal.pone.0018720 (2011).

18 Hermsen, C., van de Wiel, T., Mommers, E., Sauerwein, R. & Eling, W. Depletion of CD4+ or CD8+ T-cells prevents Plasmodium berghei induced cerebral malaria in end-stage disease. *Parasitology* **114 (Pt 1)**, 7-12 (1997).

19 Schumak, B. *et al.* Specific depletion of Ly6C(hi) inflammatory monocytes prevents immunopathology in experimental cerebral malaria. *PLoS One* **10**, e0124080, doi:10.1371/journal.pone.0124080 (2015).

20 Bongfen, S. E. *et al.* An N-Ethyl-N-Nitrosourea (ENU)-Induced Dominant Negative Mutation in the JAK3 Kinase Protects against Cerebral Malaria. *PloS one* **7**, e31012, doi:10.1371/journal.pone.0031012 (2012).

21 Gillen, C. M., Brill, S., Payne, J. A. & Forbush, B., 3rd. Molecular cloning and functional expression of the K-Cl cotransporter from rabbit, rat, and human. A new member of the cation-chloride cotransporter family. *J Biol Chem* **271**, 16237-16244 (1996).

22 Hanum, P. S., Hayano, M. & Kojima, S. Cytokine and chemokine responses in a cerebral malaria-susceptible or -resistant strain of mice to Plasmodium berghei ANKA infection: early chemokine expression in the brain. *Int Immunol* **15**, 633-640 (2003).

23 Lacerda-Queiroz, N. *et al.* Inflammatory changes in the central nervous system are associated with behavioral impairment in Plasmodium berghei (strain ANKA)-infected mice. *Exp Parasitol* **125**, 271-278, doi:10.1016/j.exppara.2010.02.002 (2010).

24 Yanez, D. M., Manning, D. D., Cooley, A. J., Weidanz, W. P. & van der Heyde, H. C. Participation of lymphocyte subpopulations in the pathogenesis of experimental murine cerebral malaria. *J Immunol* **157**, 1620-1624 (1996).

25 Amani, V. *et al.* Involvement of IFN-gamma receptor-medicated signaling in pathology and anti-malarial immunity induced by Plasmodium berghei infection. *Eur J Immunol* **30**, 1646-1655, doi:10.1002/1521-4141(200006)30:6<1646::AID-IMMU1646>3.0.CO;2-0 (2000).

26 Grau, G. E. *et al.* Tumor necrosis factor (cachectin) as an essential mediator in murine cerebral malaria. *Science* **237**, 1210-1212 (1987).

27 Kossodo, S. *et al.* Interleukin-10 modulates susceptibility in experimental cerebral malaria. *Immunology* **91**, 536-540 (1997).

28 Koch, O. *et al.* IFNGR1 gene promoter polymorphisms and susceptibility to cerebral malaria. *J Infect Dis* **185**, 1684-1687, doi:JID010716 [pii] 10.1086/340516 (2002).

29 Hill, A. V. *et al.* Common west African HLA antigens are associated with protection from severe malaria. *Nature* **352**, 595-600, doi:10.1038/352595a0 (1991).

30 Cortes, A., Benet, A., Cooke, B. M., Barnwell, J. W. & Reeder, J. C. Ability of Plasmodium falciparum to invade Southeast Asian ovalocytes varies

between parasite lines. *Blood* **104**, 2961-2966, doi:10.1182/blood-2004-06-2136 (2004).

31 Fischer, P. R. & Boone, P. Short report: severe malaria associated with blood group. *Am J Trop Med Hyg* **58**, 122-123 (1998).

32 Fry, A. E. *et al.* Common variation in the ABO glycosyltransferase is associated with susceptibility to severe Plasmodium falciparum malaria. *Hum Mol Genet* **17**, 567-576, doi:10.1093/hmg/ddm331 (2008).

33 Simpson, J. A., Aarons, L., Collins, W. E., Jeffery, G. M. & White, N. J. Population dynamics of untreated Plasmodium falciparum malaria within the adult human host during the expansion phase of the infection. *Parasitology* **124**, 247-263 (2002).

34 Kan, X. H. *et al.* Kv1.3 potassium channel mediates macrophage migration in atherosclerosis by regulating ERK activity. *Arch Biochem Biophys* **591**, 150-156, doi:10.1016/j.abb.2015.12.013 (2016).

35 Dunst, J., Kamena, F. & Matuschewsk, K. Cytokines and Chemokines in Cerebral Malaria Pathogenesis. *Front Cell Infect Mi* **7**, doi:ARTN 324 10.3389/fcimb.2017.00324 (2017).

36 Hunt, N. H. & Grau, G. E. Cytokines: accelerators and brakes in the pathogenesis of cerebral malaria. *Trends Immunol* **24**, 491-499, doi:10.1016/S1471-4906(03)00229-1 (2003).

37 van Hensbroek, M. B. *et al.* The effect of a monoclonal antibody to tumor necrosis factor on survival from childhood cerebral malaria. *J Infect Dis* **174**, 1091-1097 (1996).

38 Engwerda, C. R. *et al.* Locally up-regulated lymphotoxin alpha, not systemic tumor necrosis factor alpha, is the principle mediator of murine cerebral malaria. *J Exp Med* **195**, 1371-1377 (2002).

39 Hunt, N. H. *et al.* Cerebral malaria: gamma-interferon redux. *Front Cell Infect Microbiol* **4**, 113, doi:10.3389/fcimb.2014.00113 (2014).

40 Delpire, E. & Kahle, K. T. The KCC3 cotransporter as a therapeutic target for peripheral neuropathy. *Expert Opin Ther Targets* **21**, 113-116, doi:10.1080/14728222.2017.1275569 (2017).

41 Yamada, K. *et al.* Small-molecule WNK inhibition regulates cardiovascular and renal function. *Nat Chem Biol* **12**, 896-898, doi:10.1038/nchembio.2168 (2016).

42 Lelliott, P. M., Lampkin, S., McMorran, B. J., Foote, S. J. & Burgio, G. A flow cytometric assay to quantify invasion of red blood cells by rodent Plasmodium parasites in vivo. *Malar J* **13**, 100, doi:10.1186/1475-2875-13-100 (2014).

598 **Figure 1: The Kcc1^{M935K} mutation causes resistance to *P. berghei*. (A)** and
599 **(B)** Cumulative survival and average ± SEM parasitemia for WT and
600 Kcc1$^{M935K/M935K}$ in male mice. WT n=28, WT Kcc1$^{M935K/M935K}$ n=14. Combined
601 results of two independent experiments. **(C)** and **(D)** Cumulative survival and
602 average ± SEM parasitemia for WT and Kcc1$^{M935K/M935K}$ in female mice. WT n=8,
603 Kcc1$^{M935K/M935K}$ n=10. Combined results of two independent experiments.
604 *P<0.05, **P<0.01, ***P<0.001. P values calculated using Log rank test or the
605 student's T-test. **(E)** average ± SEM percentage of parasites which are TUNEL
606 positive. **(F)** and **(G)** Average ± SEM fold change in parasitemia and percentage
607 of remaining Kcc1$^{M935K/M935K}$ labelled cells compared to WT labelled cells injected
608 into the same *P. berghei* infected host (n=8) from 30 minutes to 21 hours post
609 inoculation. **(H)** and **(I)** Cumulative survival and average ± SEM parasitemia for
610 WT and Kcc1$^{M935K/M935K}$ in female mice in challenge where WT did not develop
611 CM. WT n=7, Kcc1$^{M935K/M935K}$ n=5.

612

613 **Figure 2: The Kcc1^{M935K} mutation causes resistance to cerebral malaria. (A)**
614 Clinical score for WT (n=37) and Kcc1$^{M935K/M935K}$ (n=24) mice infected with
615 *P. berghei* 0= no symptoms, 1= reduced movement, 2= rapid breathing/hunched
616 posture, 3= ruffled fur/external bleeding, 4= fitting/coma, 5= death. **(B)** Amount
617 of Evan's Blue dye extracted from *P. berghei* infected Kcc1$^{M935K/M935K}$ (n=8), WT
618 (n=7) and uninfected (n=4) brains. **(C)** Representative brains dissected from
619 mice injected with Evan's Blue dye. **(D)** Relative amount of *P. berghei* 18s RNA
620 normalized to mouse GAPDH in brain, spleen, and blood of infected
621 Kcc1$^{M935K/M935K}$ (n=4), WT (n=4). **(E)** Relative proportion of *P. berghei* infected

622 Red Blood Cells in the brain from flow cytometry analysis. The population was
623 gated on TER119 and Hoescht 33352 positivity. A comparison of the infected RBC
624 (iRBC) in the brain of female WT and Kcc1$^{M935K/M935K}$ mice, as an average percentage
625 of total RBC in the brain ± SEM. Uninfected controls show low background staining
626 as quantified using FACS. Uninfected WT and Kcc1$^{M935K/M935K}$ n=3. Infected WT and
627 Kcc1$^{M935K/M935K}$ n=4.Values are average ± SEM. *P<0.05, **P<0.01, ***P<0.001. P
628 values calculated using multiple T test with Two-stage linear step-up procedure
629 of Benjamin, Krieger ad Yekutieli with Q=1% (A), or ordinary one-way ANOVA
630 (B).
631
632 **Figure 3: The Kcc1^{M935K} mutation protects the brain against parasitized**
633 **RBCs.** H&E stained brain sections from representative **(I)** uninfected WT, **(II)**
634 infected WT, **(III)** uninfected Kcc1$^{M935K/M935K}$, and **(IV)** infected Kcc1$^{M935K/M935K}$
635 mice. The orange arrow indicates the presence of hemozoin pigmentation within the
636 RBCs. Sections are 20x magnification, insets are 1.25x magnification.
637
638
639 **Figure 4: The Kcc1^{M935K} mutation alters CD4+ and CD8+ T Cell populations**
640 **in the brain.** Numbers of total cells in the brain that are **(A)** CD3+CD4+ and **(B)**
641 CD3+CD8+ in uninfected WT and Kcc1$^{M935K/M935K}$ (n=3), and *P. berghei* infected
642 WT and Kcc1$^{M935K/M935K}$ (n=4). Numbers of total cells in the blood that are **(C)**
643 CD3+CD4+ and **(D)** CD3+CD8+ in uninfected WT and Kcc1$^{M935K/M935K}$ (n=3), and
644 *P. berghei* infected WT and Kcc1$^{M935K/M935K}$ (n=4). Graph shows average ± SEM.
645 *P<0.05, **P<0.01, ****P<0.0001. P values calculated using ordinary one way
646 ANOVA.

Figure 5: The Kcc1^{M935K} mutation increases pro-inflammatory cytokines in the brain. Average ± SEM amount of **(A)** TNF-α **(B)** IL-1β, and **(C)** INF-γ as measured by ELISA, in the brain and blood of uninfected WT and Kcc1$^{M935K/M935K}$ (n=3), and *P. berghei* infected WT and Kcc1$^{M935K/M935K}$ (n=4). *P<0.05, **P<0.01 P values calculated using student's T-test.

Figure S1: The M935K mutation causes an abnormal WBC response to infection. Representative H&E stained spleen sections from **(A)** uninfected WT, **(B)** infected WT, **(C)** uninfected Kcc1$^{M935K/M935K}$, and **(D)** infected Kcc1$^{M935K/M935K}$ mice. Sections are at 5x magnification; insets at 0.625x magnification.

Figure S2: The Kcc1^{M935K} mutation does not alter immune cell populations in the blood, spleen, or thymus. (A) Average ± SEM proportion of lymphocytes that are CD3+, CD11c+, and CD19+ in the blood spleen and thymus. **(B)** Average ± SEM proportion of CD3+ cells that are CD4+, CD8+, and CD4+CD8+ in the blood spleen and thymus. Black circles = uninfected WT (n=5), grey circles = uninfected Kcc1$^{M935K/M935K}$ (n=5), black open squared = infected WT (n=3), grey open squares = infected Kcc1$^{M935K/M935K}$ (n=3).

Figure S3: The Kcc1^{M935K} mutation alters the inflammatory response to *P. berghei* infection. Average ± SEM concentration of cytokines in the plasma of

672 WT and Kcc1$^{M935K/M935K}$ mice during infection with *P. berghei*. **P<0.01,

673 Significance calculated using unpaired t test

674

675

676

677

678

679

680

681

682

683 **Figure 1**

684

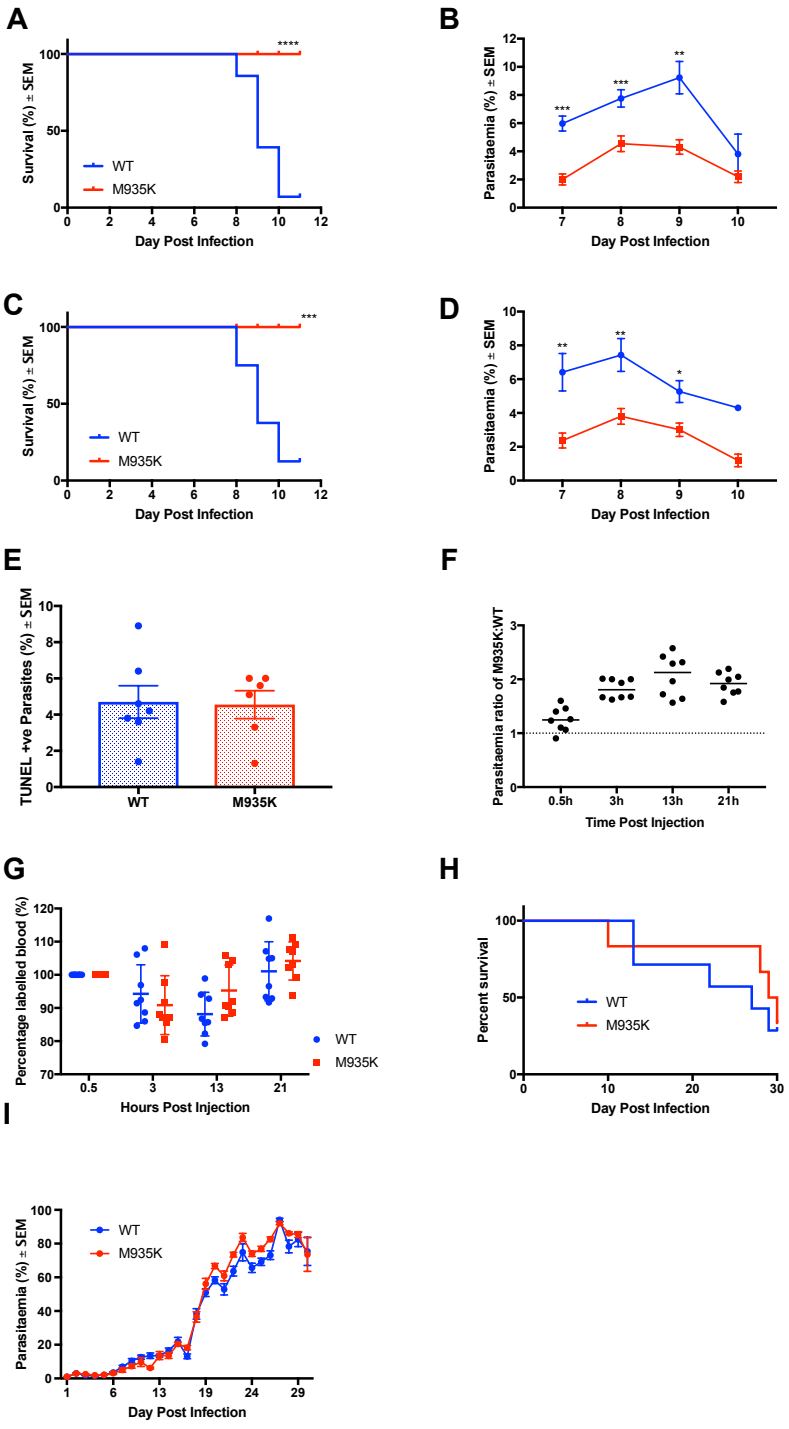

685

686 **Figure 2**

687

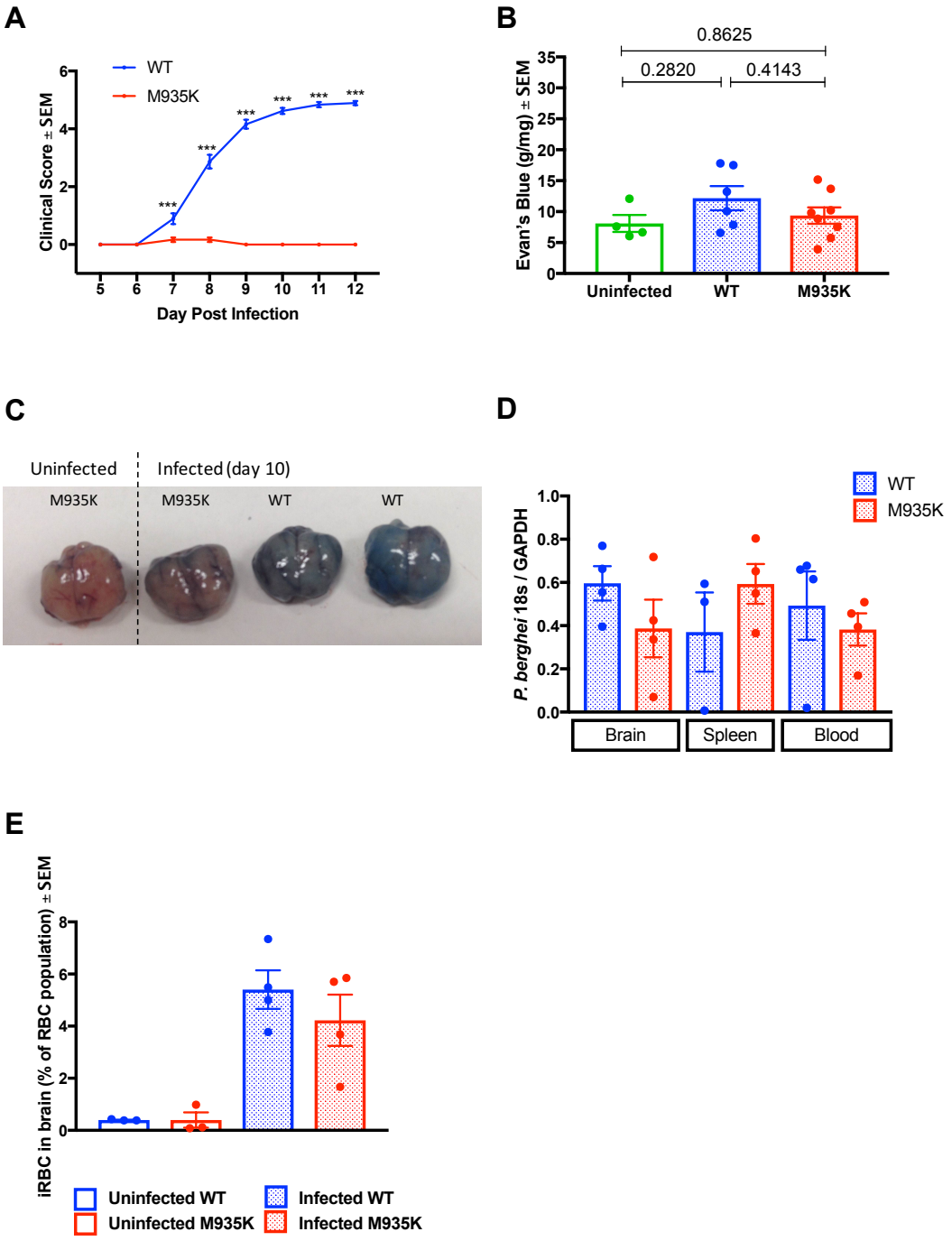

688

689

690

Figure 3

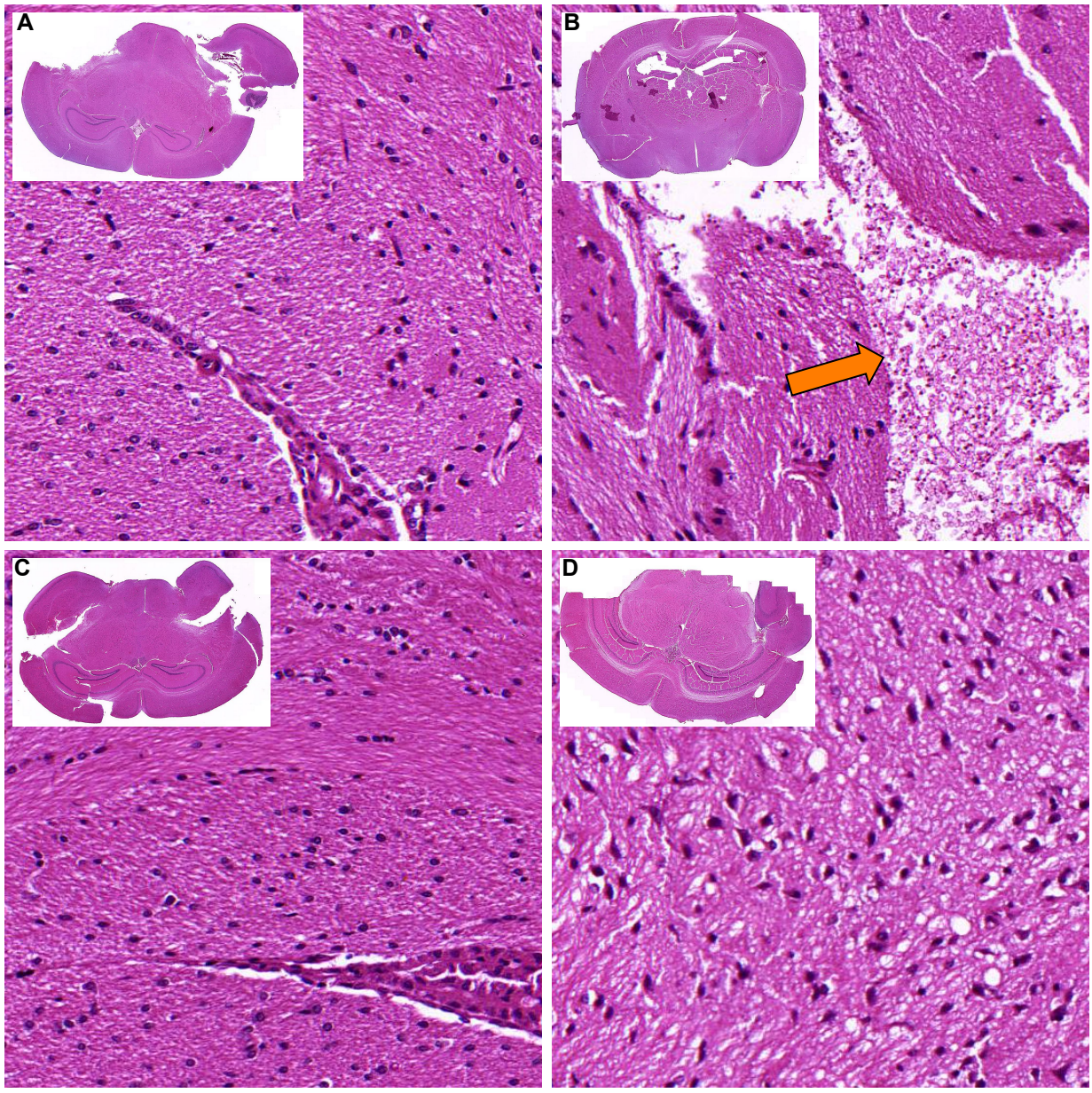

707 **Figure 4**

708

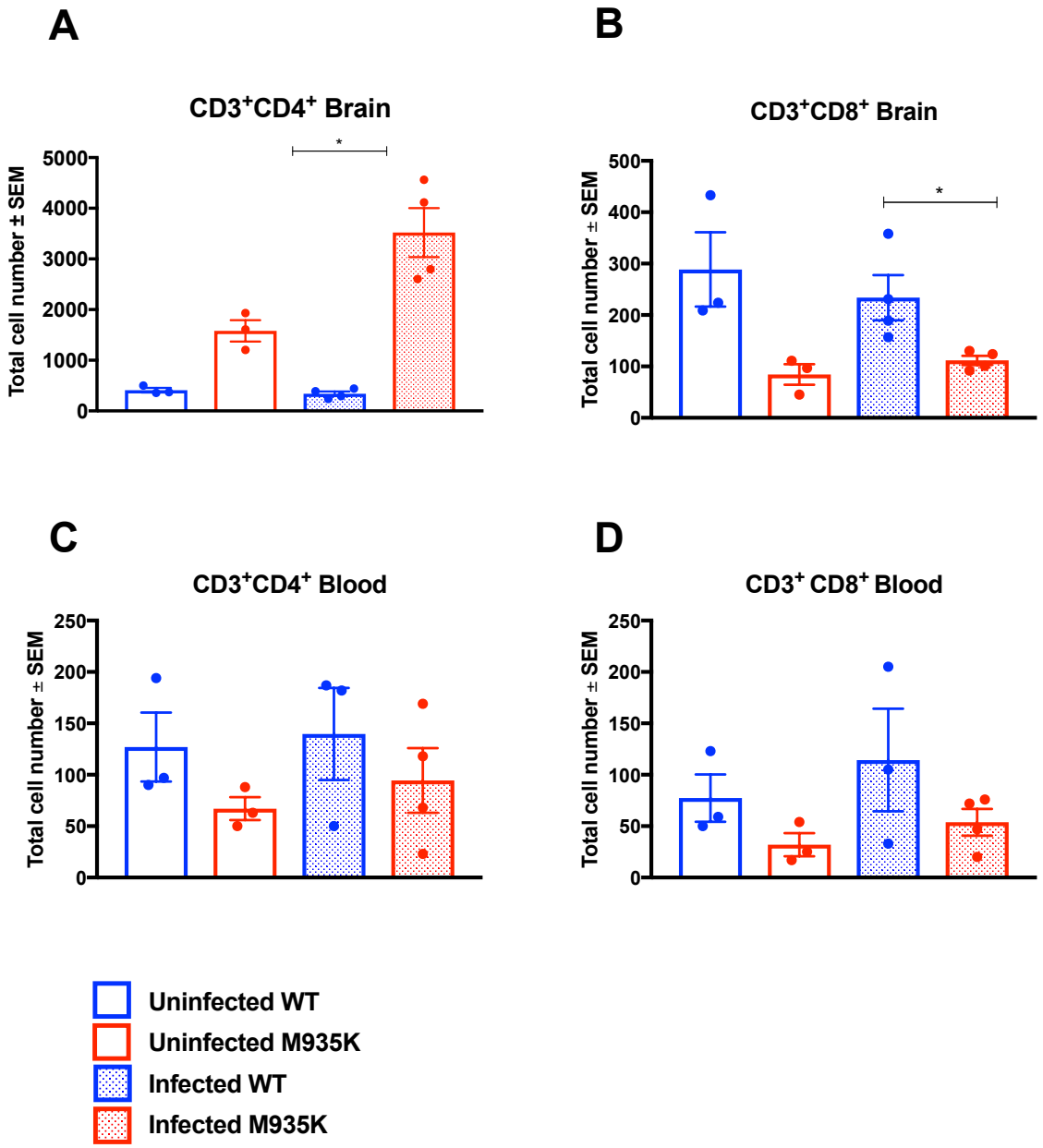

709

710

Figure 5

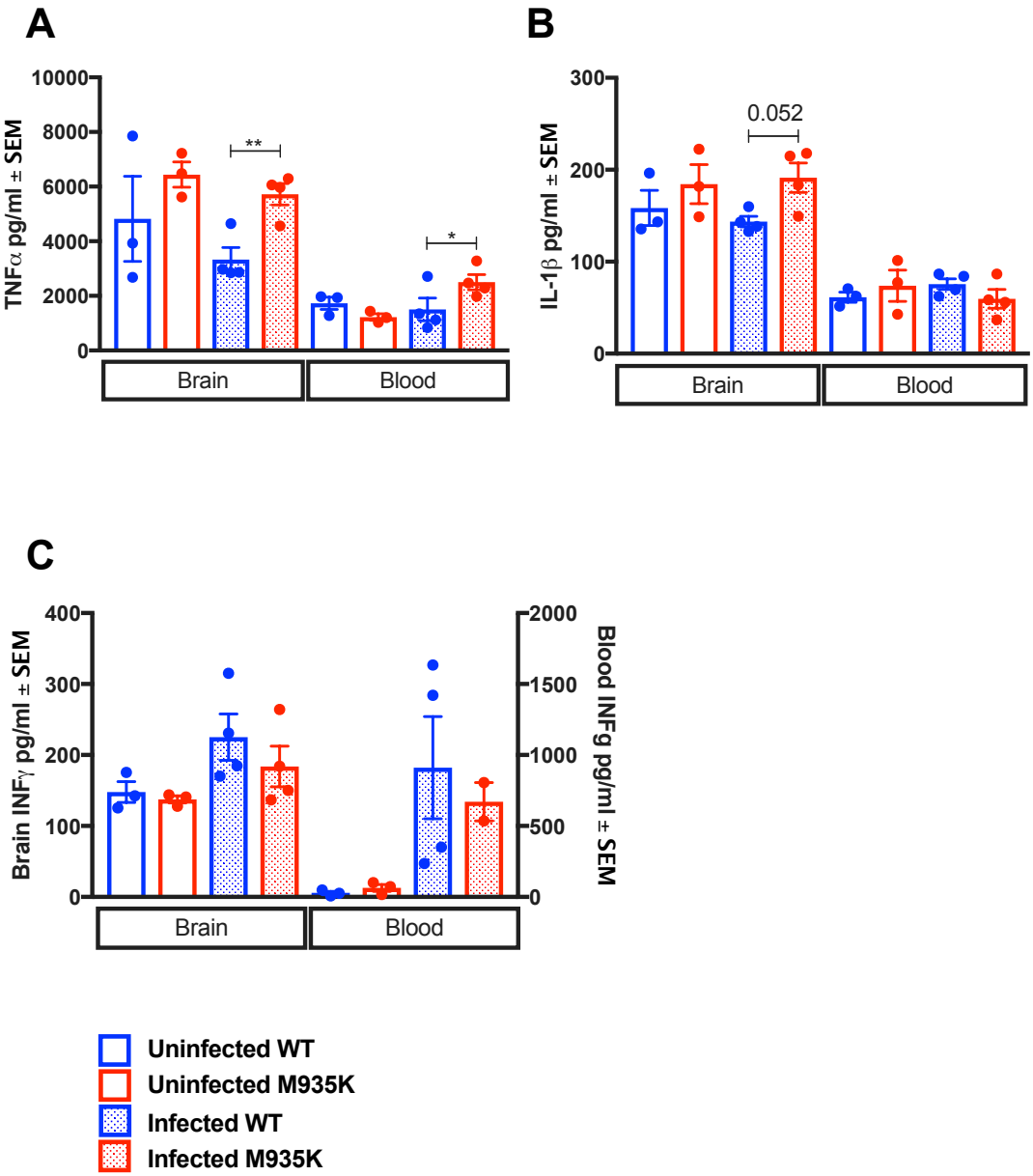
A
TNFα pg/ml ± SEM
10000
8000
6000
4000
2000
0
**
*
Brain
Blood
B
IL-1β pg/ml ± SEM
300
200
100
0
0.052
Brain
Blood
C
Brain INFγ pg/ml ± SEM
400
300
200
100
0
Blood INFg pg/ml ± SEM
2000
1500
1000
500
0
Brain
Blood
Uninfected WT
Uninfected M935K
Infected WT
Infected M935K

Supplementary material for

KCC1 Activation protects Mice from the Development of Experimental Cerebral Malaria.

Elinor Hortle[1*], Lora Starrs[1*], Fiona Brown[2], Stephen Jane[2,4,5], David Curtis[2,4], Brendan J. McMorran[1], Simon J. Foote[1], and Gaetan Burgio[1]

Figure S1

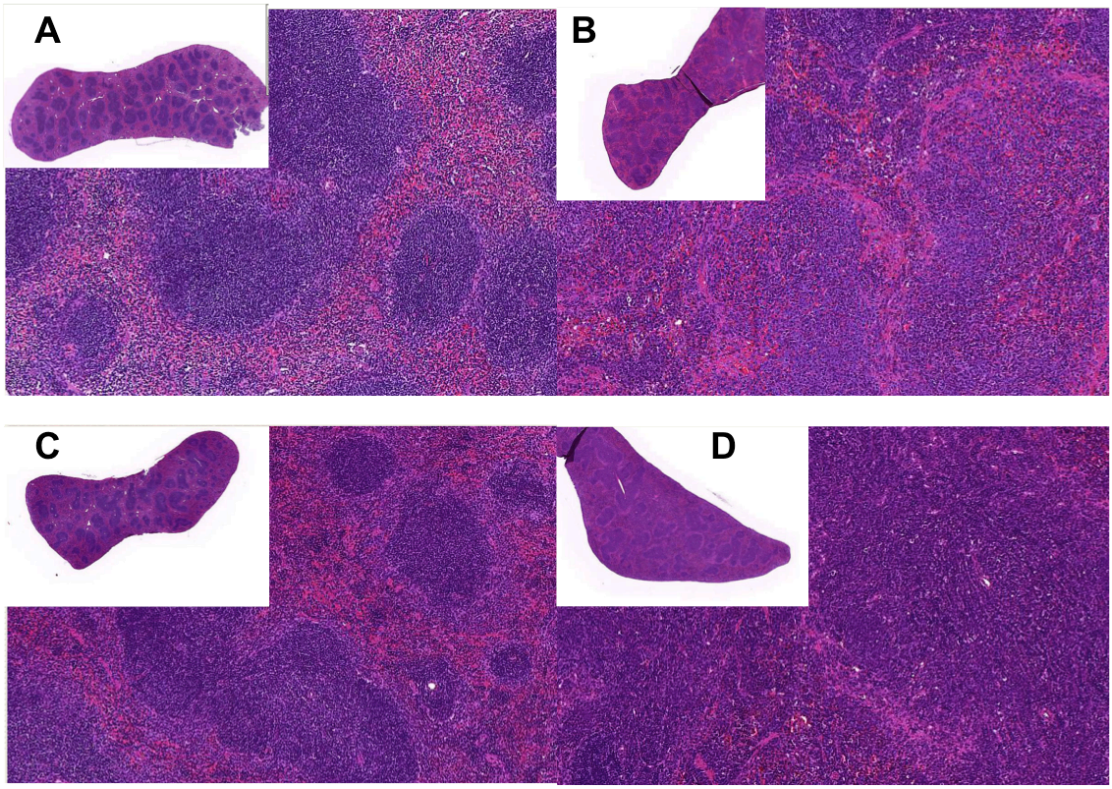

Figure S1: The M935K mutation causes an abnormal WBC response to infection. Representative H&E stained spleen sections from **(A)** uninfected WT, **(B)** infected WT, **(C)** uninfected Kcc1$^{M935K/M935K}$, and **(D)** infected Kcc1$^{M935K/M935K}$ mice. Sections are at 5x magnification; insets at 0.625x magnification.

742 **Figure S2**

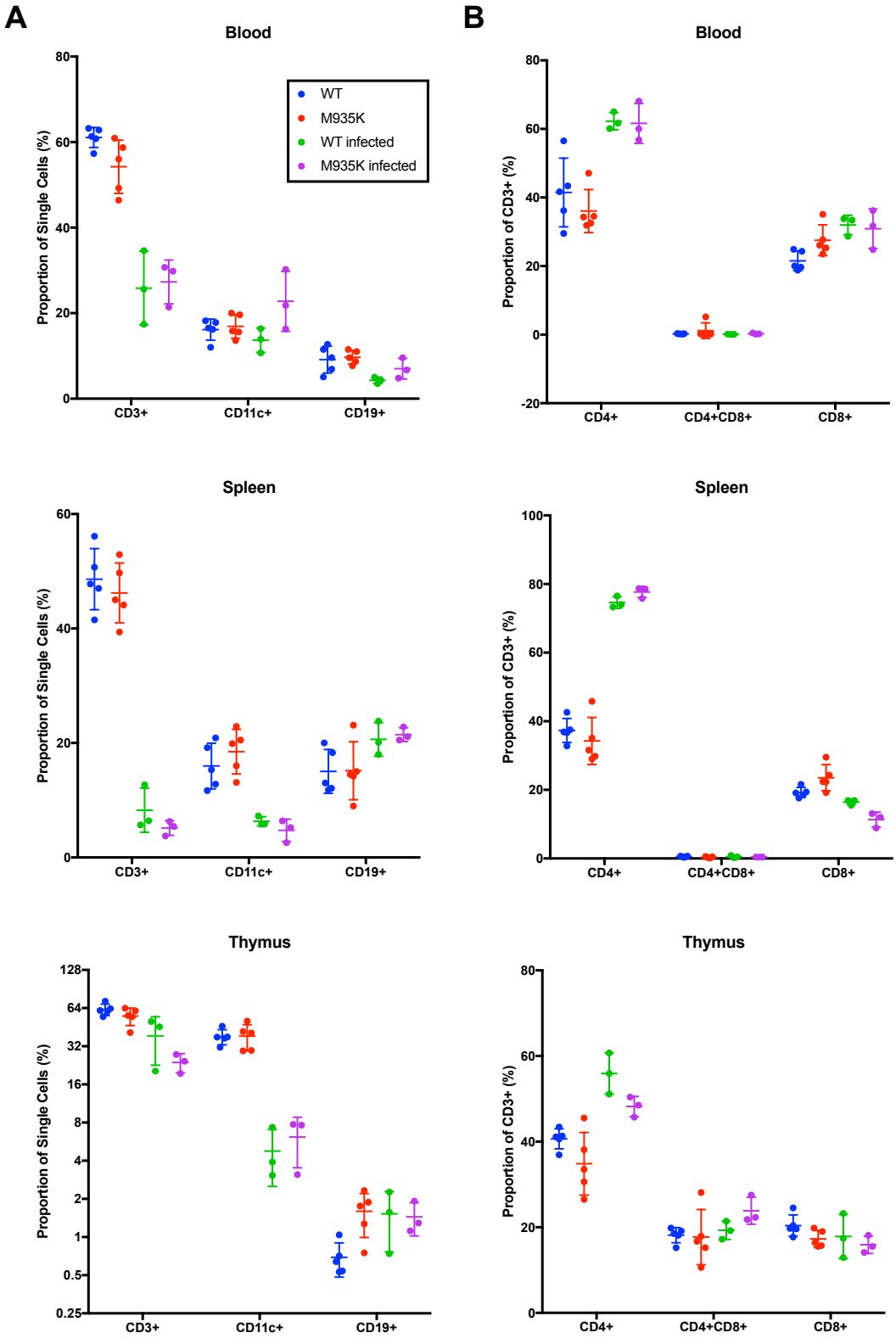

743

744

Figure S2: The Kcc1^{M935K} mutation does not alter immune cell populations in the blood, spleen, or thymus. (A) Average ± SEM proportion of lymphocytes that are CD3+, CD11c+, and CD19+ in the blood spleen and thymus. **(B)** Average ± SEM proportion of CD3+ cells that are CD4+, CD8+, and CD4+CD8+ in the blood spleen and thymus. Black circles = uninfected WT (n=5), grey circles = uninfected Kcc1$^{M935K/M935K}$ (n=5), black open squared = infected WT (n=3), grey open squares = infected Kcc1$^{M935K/M935K}$ (n=3).

Figure S3

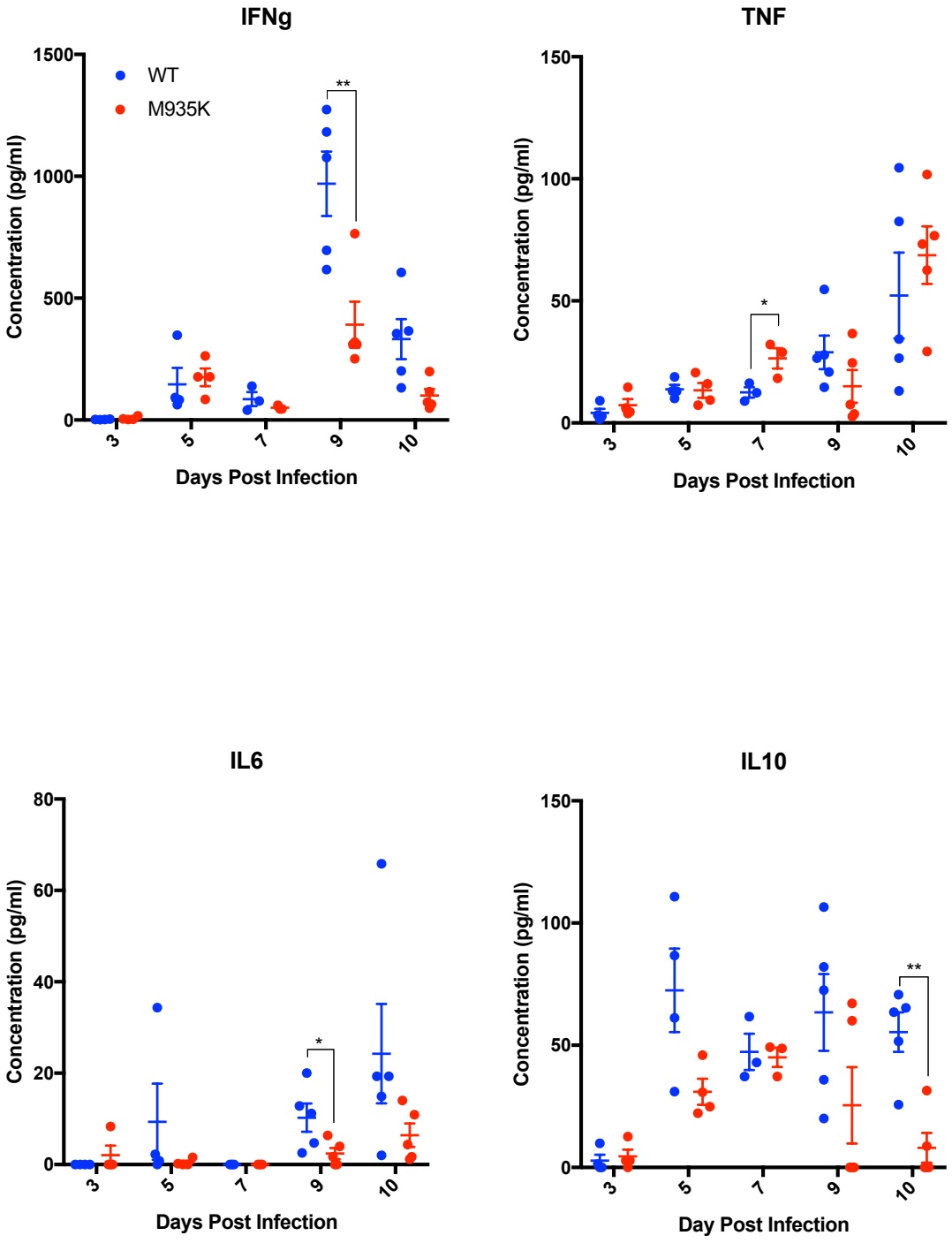

Figure S3: The Kcc1^{M935K} mutation alters the inflammatory response to *P. berghei* infection. Average ± SEM concentration of cytokines in the plasma of WT and Kcc1$^{M935K/M935K}$ mice during infection with *P. berghei*. **P<0.01, Significance calculated using unpaired t test